Quantum dots for terahertz generation

2008 J. Phys.: Condens. Matter 20 384211

(http://iopscience.iop.org/0953-8984/20/38/384211)

J. Phys.: Condens. Matter **20** (2008) 384211 (5pp) doi:10.1088/0953-8984/20/38/384211

Quantum dots for terahertz generation

H C Liu, B Aslan, J A Gupta, Z R Wasilewski, G C Aers, A J SpringThorpe and M Buchanan

Institute for Microstructural Sciences, National Research Council, Ottawa, K1A 0R6, Canada

E-mail: h.c.liu@nrc.ca

Received 18 March 2008
Published 21 August 2008
Online at stacks.iop.org/JPhysCM/20/384211

Abstract

Nanostructures made of semiconductors, such as quantum wells and quantum dots (QD), are well known, and some have been incorporated in practical devices. Here we focus on novel structures made of QDs and related devices for terahertz (THz) generation. Their potential advantages, such as low threshold current density, high characteristic temperature, increased differential gain, etc, make QDs promising candidates for light emitting applications in the THz region. Our idea of using resonant tunneling through QDs is presented, and initial results on devices consisting of self-assembled InAs QDs in an undoped GaAs matrix, with a design incorporating a GaInNAs/GaAs short period superlattice, are discussed. Moreover, shallow impurities are also being explored for possible THz emission: the idea is based on the tunneling through bound states of individual donor or acceptor impurities in the quantum well. Initial results on devices having an AlGaAs/GaAs double-barrier resonant tunneling structure are discussed.

1. Introduction

The terahertz (THz) frequency range of the electromagnetic spectrum is very much under-utilized mainly because of the lack of convenient sources and detectors. Towards the realization of both detectors and emitters operating in the THz, semiconductor nanostructures, such as quantum wells (QW) and quantum dots (QD), have drawn a lot of attention ([1–3], and references therein). In spite of the fact that QD studies are not currently as well established as those of quantum wells, their potential advantages like low threshold current density, high characteristic temperature, increased differential gain, etc make them promising candidates for THz generation ([4, 5] and references therein). Here, we present our idea of THz generation using resonant tunneling (RT) structures with two different approaches: self-assembled InAs QDs and shallow impurities. Initial results on resonant tunneling through QDs and impurities are discussed. We stress that we are at the very beginning of this research and its eventual success would require a dedicated systematic effort and a visionary funding source.

2. Resonant tunneling through quantum dots

The conduction band intersublevel separations in self-assembled InAs quantum dots in GaAs matrix match the THz region, and they are therefore naturally suited for THz

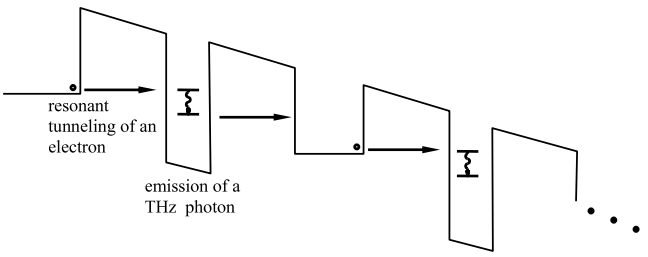

Figure 1. Schematic representation of 'quantum cascade' emission.

generation: one possible approach, as shown in figure 1, is to use 'quantum cascade' (QC) structure where once an electron has undergone an intersublevel transition and emitted a photon in one period, it tunnels into the next period of the structure where another photon can be emitted. This process of a single electron causing the emission of multiple photons as it traverses through the QC laser (QCL) structure makes a quantum efficiency of greater than unity possible which leads to higher output powers than for conventional semiconductor laser diodes.

The first step for implementing the concept is studying resonant tunneling through QDs [6] in a design schematically shown in figure 2: the QD layer surrounded by undoped GaAs barriers is clad by two n-GaInNAs regions which serve as the injector and collector of electrons. In order to inject electrons directly into the QD states with sufficient voltage tunability,

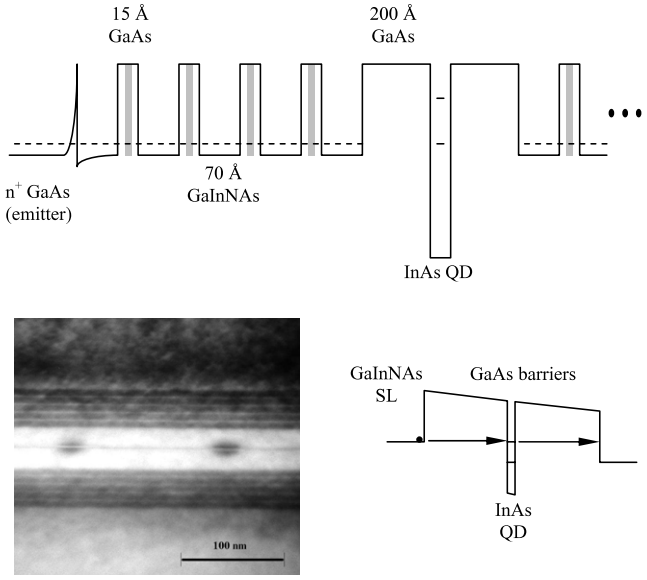

Figure 2. Schematic representation of the structure grown (top) and tunneling process; under appropriate bias electrons resonantly tunnel through the dot layer (down right). TEM image (bottom left) showing the QDs in a symmetrical superlattice structure.

the injector material must have its conduction band edge lower than the ground state of the QD. Moreover, it is preferable that the injector and collector materials are lattice matched to GaAs so that they do not influence the growth of InAs QDs. For this purpose the newly developed GaInNAs material was chosen for use as both injector and collector. For such material systems, it is crucial to avoid direct doping of GaInNAs (Si doping results in a highly resistive GaInNAs layer with a different fundamental bandgap). We therefore employed a GaAs/GaInNAs short period superlattice (SL) with modulation doping in the thin GaAs barriers as both injector and collector.

2.1. Experimental details

Samples used in this study were grown by molecular beam epitaxy (MBE) on an n^+-GaAs substrate. During the growth process, the wafer rotation was stopped in each GaInNAs layer to have a systematic set of samples in a single growth run by exploiting the natural, geometric flux gradients of the MBE system. We, thus, obtained a series of samples where the relative position of the SL state is different with respect to the QD state (due to the N gradient), which allowed us to determine the material contents in the SL for the best tunneling condition. Detailed device structure and growth conditions can be found in [7]. Transmission electron microscope (TEM) images showed the QDs with symmetrical superlattice contact layers on both sides (figure 3 (top)). Mesa devices of different sizes (from 10×10 μm^2 to 1500×1500 μm^2) were fabricated with NiGeAu ohmic contacts. I–V measurements of different size devices indicated that the material uniformity is excellent as the same current density was observed for the same N content. Larger devices have ring shaped top contacts to allow laser illumination for both electrical and optical measurements. For optical measurements, samples were mounted in a liquid nitrogen Dewar with a Pyrex window. Using a 632.8 nm HeNe laser as the excitation source, the PL spectra were collected by a Bomem DA8 Fourier transform infrared spectrometer (FTIR) with a cooled InGaAs detector.

2.2. Results and discussion

Figure 3 shows the dark current density (left) and its derivative (right) versus voltage at liquid helium temperature for samples having different N contents. The effect of the N gradient across the wafer and clear resonant tunneling features are seen: since increasing the nitrogen composition in GaInNAs for a fixed In content reduces the bandgap of the alloy, deeper wells are created in the superlattice and therefore less current passes through the device. On the other hand, tunneling occurs at different bias values for different samples because of the change in the positions of the energy states (minibands) in the superlattice. The tunneling features seen at small voltage values come from the process of resonant tunneling through the dots as shown schematically in the bottom right part of figure 2. Our theoretically calculated current–voltage curves revealed that the high voltage features are due to Fowler–Nordheim

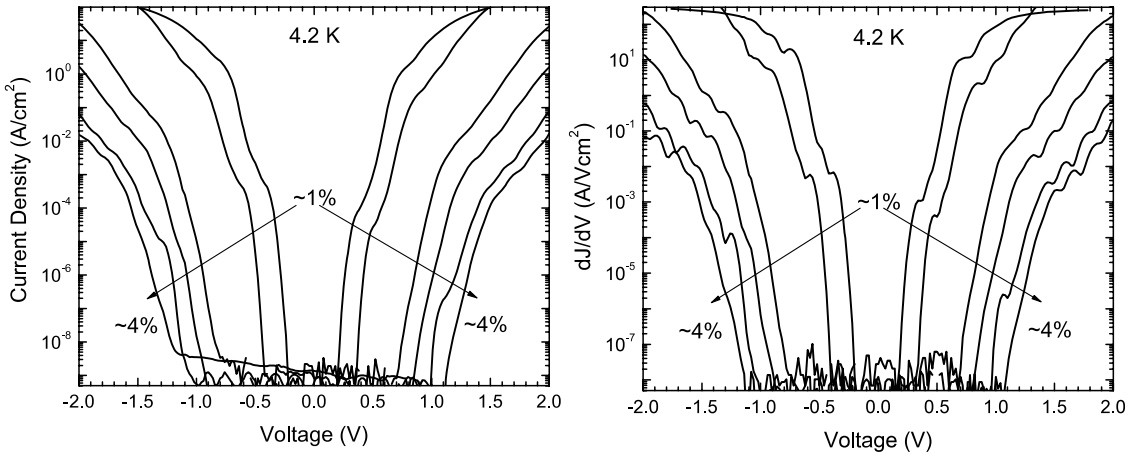

Figure 3. Dark current density (left) and its derivative (right) versus voltage curves at liquid helium temperature (4.2 K) for samples having different N contents.

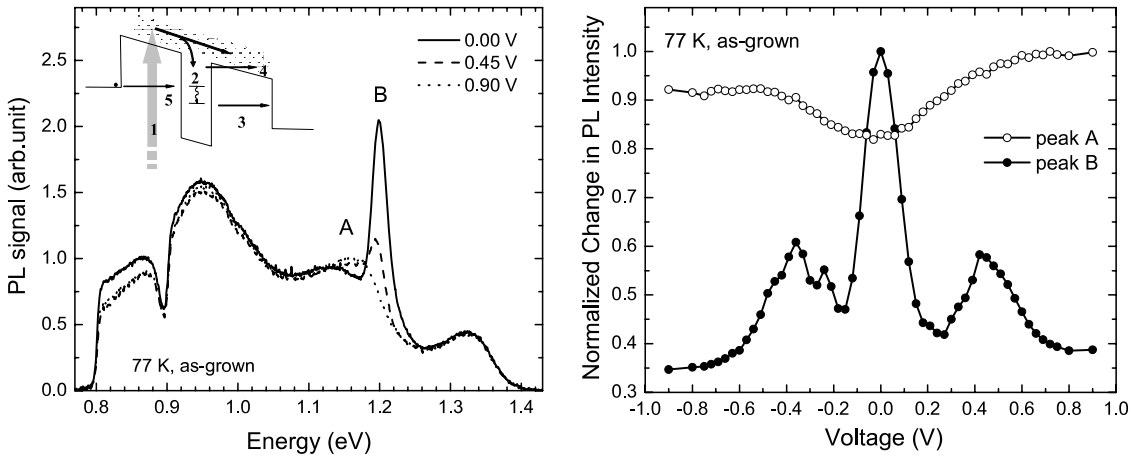

Figure 4. PL spectra for the sample having ∼1% N for different biases (left) and the change in the intensity of the PL signal originating from the QDs with applied voltage (right). The inset: schematic representation of the processes in the structure.

resonances. We, therefore, focus on the small bias region and performed other experiments to confirm that the observed features are indeed due to resonant tunneling through the dots. We also concentrate on samples with low N contents (∼1%) so that the current is high enough to be measured reliably.

Further investigations, mainly photoluminescence (PL) studies, on the sample having ∼1% N, 11% In, allowed us to understand the physical mechanisms in such structures. As shown in figure 4, PL spectra strongly depend on the applied bias on the device: two peaks originating from the QD ground and excited states show different bias dependences. With the help of applied bias, more photo-generated carriers (inset, process 1) created above the band edges can be captured into the dots, filling the states (process 2). For deeply confined ground state carriers, times for carrier tunneling escape through the GaAs barrier (process 3) remain much longer than the radiative recombination time for all values of bias, and therefore the PL signal coming from the ground state monotonically increases with increasing bias to a saturated value. On the other hand, carriers in an excited state, closer to the top of the barrier, can easily tunnel into the continuum (process 4) before they recombine with the valence band holes. Moreover, with increased bias the effective height of the tunnel barrier is reduced significantly and thus excited state carrier escape tunneling times are reduced significantly with increasing bias. When these become comparable to or shorter than the radiative lifetimes, the PL intensity of the excited states decreases. However, when the resonance condition is met, extra carriers from the SL are injected into the excited state (process 5), which increases the carrier density in the dots. This results in a rise of the PL signal at a particular voltage, while any further bias misaligns the resonant tunneling, so the signal gets smaller again as seen in figure 4 (right). Tunneling features were also evidenced by the capacitance–voltage measurements (not shown here). The features observed from the results of each technique are in good agreement with each other and they are consistent with the expectation for the resonant tunneling. On the basis of the results obtained, further characterization/optimization is needed in leading to the goal of THz emission.

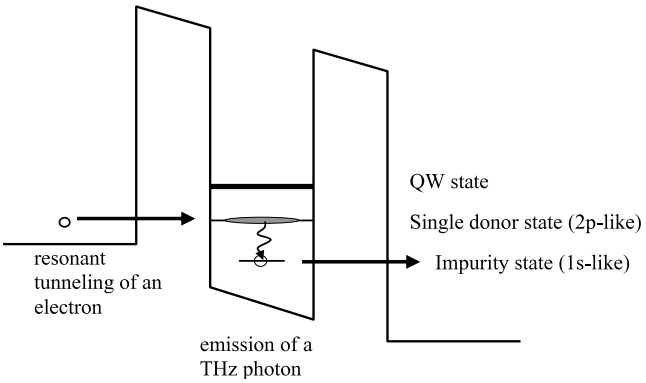

Figure 5. Schematic representation of the idea of generating THz emission by using impurity states in a resonant tunneling diode.

3. Resonant tunneling through impurity states

An alternative approach for generating THz emission is incorporating impurities as 'QDs' into a quantum well: the presence of impurities in the QW of a double-barrier resonant tunneling diode (DBRTD) gives rise to localized states below the edge of the first subband in the quantum well [8, 9] (see figure 5). In a donor-assisted tunneling process, an externally applied voltage, lower than the one necessary for the resonance of the QW first subband states, leads to the alignment of a donor state in the QW and an occupied state in the emitter. Since the impurity levels are very much like quantum dots, one would expect an electron to undergo an 'intersublevel' transition and emit a photon as schematically depicted in figure 5. The binding energies of the ground (1s-like) and excited (2p-like) states of an impurity associated with the first subband in a quantum well depend on the quantum well width, and the position of the impurity in the well, as well as the type of the impurity [8, 9]. Thus, the use of quantum wells enables tuning of the impurity level energy, so we can design QCLs in a wide range of THz frequencies. By using different impurities and n- or p-type samples, we could cover the entire THz spectrum.

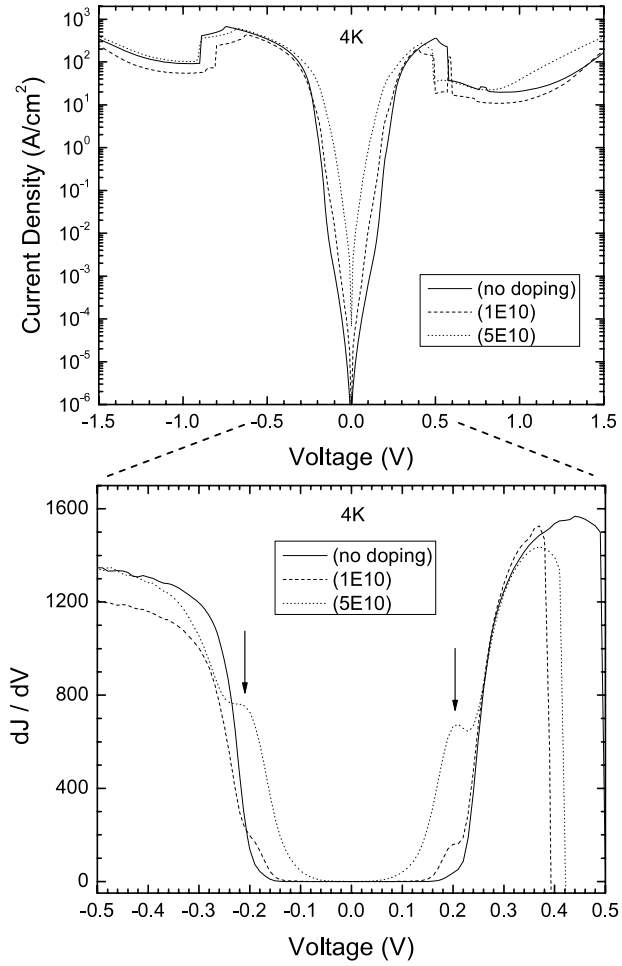

Figure 6. Current density versus voltage characteristics (top) and their derivatives (bottom) for devices with various amounts of donors incorporated at the center of the quantum well.

Table 1. Device structure and parameters for both n- and p-type samples.

	n-type sample	p-type sample
GaAs (top contact)	4000 Å (Si: 2×10^{18})	1000 Å (C: 2×10^{19})
GaAs	1000 Å (Si: 1×10^{17})	1000 Å (C: 1×10^{18})
GaAs	200 Å	100 Å
$Al_xGa_{1-x}As$ (barrier)	50 Å ($x = 0.4$)	20 Å ($x = 1$)
GaAs (well)	60 Å	40 Å
δ doping	(Si: various)	(C: various)
$Al_xGa_{1-x}As$ (barrier)	60 Å ($x = 0.4$)	25 Å ($x = 1$)
GaAs	200 Å	100 Å
GaAs	1000 Å (Si: 1×10^{17})	1000 Å (C: 1×10^{18})
GaAs (bottom contact)	7000 Å (Si: 2×10^{18})	6000 Å (C: 2×10^{19})
SI GaAs substrate		
	δ doping: none, 1×10^{10},	5×10^{10} cm^{-2}

3.1. Experimental details

As in the quantum dot case, the first step is to observe the resonant tunneling thorough the impurity states; in this respect, we have investigated n-type (Si doping) MBE grown AlGaAs/GaAs/AlGaAs and p-type (Be doping) MOCVD grown AlAs/GaAs/AlAs double-barrier resonant tunneling diodes. The device structure and parameters, i.e. layer thicknesses, doping levels etc, are given in table 1. Note that the above mentioned impurity states were incorporated into the system by delta doping the quantum well at the center. Tunneling thorough impurity states was evidenced for both n- and p-type samples in electrical measurements.

3.2. Results and discussion

Figure 6 shows current–voltage characteristics for devices with different levels of doping (n-type) and their derivatives (bottom) to reveal the features more clearly. In order to confirm

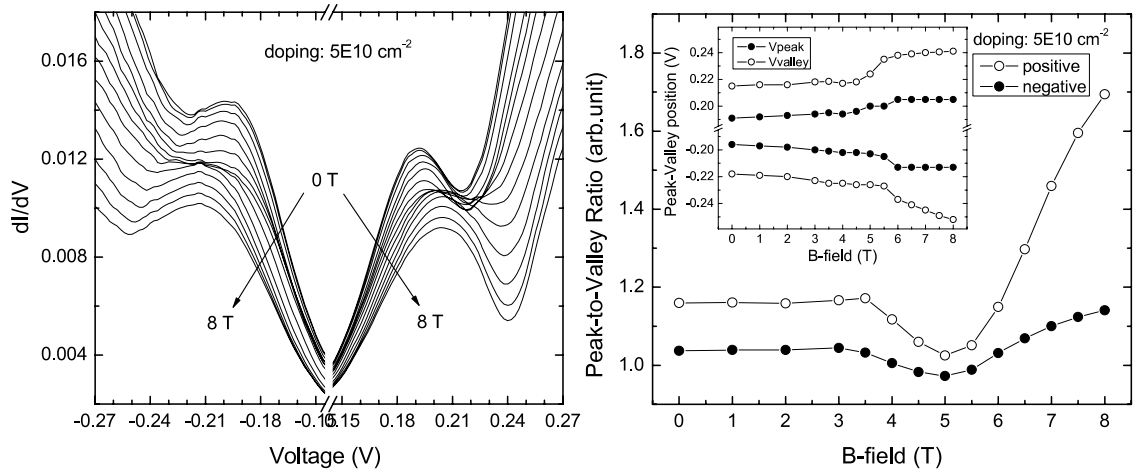

Figure 7. Effect of the magnetic field on the resonant tunneling feature indicated in figure 6 (bottom): change in current with voltage in the region of interest (left) and the corresponding peak to valley ratio for each magnetic field (right). The inset shows the shift in peak and valley positions with magnetic field.

the observed features in I–V graphs and to have a better understanding, we checked the current–voltage characteristics under magnetic field. For a magnetic field along the current flowing in the structure (i.e. growth direction), the electron motion in the QW plane is quantized into Landau levels. Thus, not only the binding energy but also the energy separation between the 1s-like ground state and the 2p-like excited state increases with increasing magnetic field strength. The effect of the magnetic field on the resonant tunneling feature observed in I–V (indicated by arrows in figure 6 (bottom)) is shown in figure 7. To quantify the effect, the peak to valley ratio for each magnetic field value was plotted (figure 7 (right)). Generally the ratio is enhanced at high magnetic field, indicating an enhanced resonant tunneling. This is expected due to the Landau level 'confinement'. Before the enhancement, a slight suppression of the feature around 5 T is observed. The reason for this needs to be investigated further. Similar but less clear effects were obtained for p-type samples.

4. Conclusion

To conclude, we have made initial progress towards making a QD or impurity THz emitter. Resonant tunnelings through both QDs and impurities are observed. Substantially more work is required to reach our final goal and realize the projected advantages [10].

References

[1] Liu H C, Luo H, Ban D, Wächter M, Song C Y, Wasilewski Z R, Buchanan M, Aers G C, SpringThorpe A J, Cao J C, Feng S L, Williams B S and Hu Q 2006 *Chin. J. Semicond.* **27** 627
[2] Wasserman D, Gmachl C, Lyon S A and Shaner E A 2006 *Appl. Phys. Lett.* **88** 191118
[3] Ryzhii V 1996 *Semicond. Sci. Technol.* **11** 759
[4] Hsu C-F, O J-S, Zory P and Botez D 2000 *IEEE J. Sel. Top. Quantum Electron.* **6** 491
[5] Ledentsov N N, Ustinov V M, Shchukin V A, Kopev P S, Alferov Z I and Bimberg D 1998 *Semiconductors* **32** 343
[6] Luyken R J, Lorke A, Govorov A O, Kotthaus J P, Ribeiro G M and Petroff P M 1999 *Appl. Phys. Lett.* **74** 2486
[7] Aslan B, Liu H C, Gupta J A, Wasiliewski Z R, Aers G C, Raymond S and Buchanan M 2006 *Appl. Phys. Lett.* **88** 043103
[8] Bastard G 1981 *Phys. Rev.* B **24** 4714
[9] Greene R L and Bajaj K K 1985 *Phys. Rev.* B **31** 913
[10] Dmitriev I A and Suris R A 2008 *Physica* E at press